Carbohydrate Polymers 114 (2014) 78–86

Contents lists available at ScienceDirect

Carbohydrate Polymers

journal homepage: www.elsevier.com/locate/carbpol

Novel pH-responsive dextrin nanogels for doxorubicin delivery to cancer cells with reduced cytotoxicity to cardiomyocytes and stem cells

Somkamol Manchun[a,b], Kamonrak Cheewatanakornkool[a,b], Crispin R. Dass[c,d], Pornsak Sriamornsak[a,b,*]

[a] Department of Pharmaceutical Technology, Faculty of Pharmacy, Silpakorn University, Nakhon Pathom 73000, Thailand
[b] Pharmaceutical Biopolymer Group (PBiG), Faculty of Pharmacy, Silpakorn University, Nakhon Pathom 73000, Thailand
[c] School of Pharmacy, Faculty of Health Sciences, Curtin University, Bentley 6102, Australia
[d] Biosciences Research Precinct, Curtin University, Bentley 6102, Australia

ARTICLE INFO

Article history:
Received 21 April 2014
Received in revised form 27 June 2014
Accepted 3 August 2014
Available online 10 August 2014

Keywords:
pH-responsive
Nanogels
Dextrin
Doxorubicin
Cancer

ABSTRACT

The aim of this study was to develop pH-responsive dextrin nanogels (DNGs) capable of triggered intracellular DOX release at the lower pH of cancer cells. DNGs were prepared by an emulsion cross-linking method using glyoxal as cross-linker to create an acid-labile bond. A higher molecular weight of dextrin with increasing mole ratio of dextrin to glyoxal decreased the average diameter of DNGs. DNGs showed slightly negative surface charge and pH-responsive behavior. The in vitro drug release was slow at pH 7.4 and increased with decreasing pH (pH 5 > 6.8). The cytotoxicity of DOX-loaded DNGs in mesenchymal stem cells and cardiomyocytes was lower than that of free DOX. Moreover, DOX-loaded DNGs were efficiently internalized by tumor cells with rapid release of DOX into the nucleus. Thus, DOX-loaded DNGs were successful for intracellular targeted anti-tumor drug delivery and reducing side-effects to non-tumor cells such as cardiomyocytes and stem cells.

1. Introduction

Doxorubicin (DOX), one of the most commonly used anticancer drugs in chemotherapy, has a high anti-tumor activity against hematopoietic malignancies and solid tumors such as hepatocellular, breast, ovarian, bladder, and gastric cancers (Arif, Hooper, Greco, Williams, & Boateng, 2013; Weng, Le, Lin, & Golzarian, 2011). However, DOX exhibits dose-dependent cardiotoxicity which frequently leads to congestive heart failure (Gianni et al., 2008; Minotti, Menna, Salvatorelli, Cairo, & Gianni, 2004; Tacar, Sriamornsak, & Dass, 2013) due to the lack of ability to target cancer cells. In order to overcome these restrictions, nanoparticle-based stimuli-responsive carriers, have been exploited for targeting the delivery of drugs *via* the enhanced permeability and retention (EPR) concept (Maeda, Bharate, & Daruwalla, 2009; Shi, Votruba, Farokhzad, & Langer, 2010). In this concept, the nanocarriers (in the size range of 20–200 nm) extravasate through leaky tumor capillary fenestrations that result from abnormalities of angiogenesis at the tumor site, resulting in accumulation and retention (Alexis, Pridgen, Langer, & Farokhzad, 2010; Maeda, Bharate, & Daruwalla, 2009; Maeda, Sawa, & Konno, 2001). After reaching the tumor site, the drug is released from the carrier by appropriate stimuli, for example, pH, glucose, light, temperature and magnetic field (Fleige, Quadir, & Haag, 2012; Ganta, Devalapally, Shahiwala, & Amiji, 2008; Motornov, Roiter, Tokarev, & Minko, 2010). Among these stimuli, pH variation in tumor tissue and intracellular compartments have gained interest as an ideal trigger due to the fact that the pH at both primary and metastasized tumors is lower than the pH of normal tissue. The average extracellular pH value in tumor tissue is 6.8 and endosomes and lysosomes is 4.5–6.5 (Gerweck & Seetharaman, 1996).

Recently, nanogels have been investigated as pH-responsive drug carriers because of ease of synthesis, controlled size and functionalization. The pH-responsive nanogels are cross-linked polymer networks fabricated by incorporating pH-responsive polymers or pH-responsive bonds into their structure. pH-responsive bonds such as hydrozone (Bae, Fukushima, Harada, & Kataoka, 2003; Bae, Nishiyama, & Kataoka, 2007), cis-aconityl (Hu, Liu,

* Corresponding author at: Department of Pharmaceutical Technology, Faculty of Pharmacy, Silpakorn University, Nakhon Pathom 73000, Thailand.
Tel.: +66 3425 5800; fax: +66 3425 5801.
E-mail address: pornsak@su.ac.th (P. Sriamornsak).

http://dx.doi.org/10.1016/j.carbpol.2014.08.002
0144-8617/

Du, & Yuan, 2009; Yoo, Lee, & Park, 2002) and acetal (Bachelder et al., 2008) bonds are used linkers to immobilize anti-tumor drugs within the carrier matrix. As the matrix degrades in response to pH changes in the tumor environment, the drug is released. To improve biocompatibility, various biopolymers have been employed to prepare nanogels, such as chitosan, alginate and starch.

Dextrin, a saccharide-based polymer containing D-glucose units linked by α-(1→4) glycosidic bond, is produced by partial hydrolysis of starch (Carvalho, Gonçalves, Gil, & Gama, 2007). There are many reports on the use of dextrin in biomedical applications due to its biocompatibility and degradability (Carvalho et al., 2007; Ferguson & Duncan, 2009). Dextrin is a hydrophilic polymer, which contains considerable amounts of hydroxyl groups that are easy to modify. Gonçalves and Gama (2008) and Gonçalves, Martins, and Gama (2007) developed and characterized nanogels obtained by self-assembly of hydrophobically-modified dextrin. The obtained nanogels have high colloidal stability and are spherical. Moreover, the interaction with murine macrophages and blood clearance were evaluated and it was observed that the dextrin nanogel is non-cytotoxic and are phagocytosed by macrophages (Gonçalves et al., 2010). Blood clearance of the nanogels occurs in the first 3 h after intravenous administration, with about 30% remaining at this stage, then continuing slowly up to 24 h. Accordingly, with fairly high blood circulation time and biocompatibility, dextrin nanogels are promising carriers for biomedical applications. Recently, dextrin nanogels have been used for solubilization and delivery of lipophilic curcumin, improving its stability and controlling its release (Gonçalves, Pereira, Schellenberg, Coutinho, & Gama, 2012).

In this study, dextrin was used as a starting material to fabricate nanogels through an emulsion cross-linking method combined with pH-sensitive linkage (Fig. 1). We tested these dextrin nanogels (DNGs) *in vitro*. Tumor cell uptake and side-effects to normal cells were also evaluated.

2. Materials and methods

2.1. Materials

Dextrins (molecular weight (M_w) of 1400 and 1000 Da, referred as D2 and D4, respectively) were a gift from Siam Modified Starch Company Ltd. (Pathumthani, Thailand). Glyoxal, ethanol and doxorubicin hydrochloride were obtained from Sigma–Aldrich Chemie (Steinheim, Germany). Hydrochloric acid and *n*-hexane were purchased from RCI *Labscan* (Bangkok, Thailand). Tween® 80 and Span® 80 were purchased from P.C. Drug Center Co., Ltd. (Bangkok, Thailand). All reagents were of analytical or pharmaceutical grade and used as supplied without further purification. Deionized water was used throughout the study. Rat cardiomyocyte H9c2 cells were obtained from the American Tissue Culture Collection (ATCC; Manassas, VA, USA). Murine bone marrow-derived mesenchymal stem cells (MSCs) were obtained using a published procedure (Soleimani & Nadri, 2009) covered by an institutional ethics approval (Victoria University AEC approval # 16/10).

2.2. Preparation of dextrin nanogels

DOX-loaded DNGs were prepared as previously described by our group with some modifications (Fig. 2) (Manchun, Dass, & Sriamornsak, 2014). Dextrin and DOX were dissolved in the water phase to obtain the final concentration of 5% (w/w) and 0.2 mg/mL, respectively. The water phase was added to the emulsion template and ultrasonicated for 1 min to form nanoemulsions. After the nanoemulsions were homogeneously mixed, glyoxal as a cross-linker was added immediately with homogenizing *via* ultrasonication for 30 min and stirred with a magnetic stirrer for 12 h to continue the cross-linking reaction. DNGs were precipitated from the nanoemulsions by adding 99% (v/v) ethanol and washed 3 times with ethanol and finally rinsed in water. Subsequently, the DNGs were dried by vacuum freeze-drying for 24 h. The dry DNGs obtained from the vacuum freeze-drying process was packaged in zip-lock bags and kept in the refrigerator (4 °C) till further analysis.

2.3. Droplet size and ζ-potential determination

The mean droplet size and ζ-potential of the prepared nanogels were determined by dynamic light scattering at 25 °C using a Zetasizer Nano ZS (Malvern Instruments, Malvern, UK) operating at a wavelength of 623 nm and a detection angle of 173° equipped with a Peltier temperature control unit. The hydrodynamic radius of nanogels was determined with a Laplace inversion using the model-independent CONTIN program. The dispersed nanogels were filtered through a 0.45-μm membrane before measurement. The measurement of particle size and ζ-potential was performed in triplicate.

2.4. ^{1}H NMR and ^{13}C NMR

The prepared nanogels were dissolved in deuterium oxide. The ^{1}H NMR and ^{13}C NMR spectra were recorded on NMR spectroscopy (model ADVANCE 300, Bruker, Germany). The chemical shifts were given in δ (ppm).

2.5. Drug content and encapsulation efficiency

DNGs were dispersed in 1.0 N HCl and stirred for 12 h. Subsequently, the suspensions were filtered through a 0.45-μm cellulose acetate membrane. The DOX concentration in DNGs was determined by measuring UV absorbance at 495 nm with a UV/vis spectrophotometer (model T60U, PG Instrument Ltd., England). All measurements were performed in triplicate. DOX concentration was then calculated based on a standard curve of known amounts of DOX in 0.1 N HCl. Encapsulation efficiency and loading content were defined as:

$$\text{Encapsulation efficiency (\%)} = \frac{\text{Amount of drug in nanogels (mg)} \times 100}{\text{Theoretical amount of drug in nanogels (mg)}} \quad (1)$$

$$\text{Loading content (\%)} = \frac{\text{Weight of loaded drug (mg)} \times 100}{\text{Weight of drug-loaded nanoparticles (mg)}} \quad (2)$$

2.6. In vitro pH-dependent drug release

DOX-loaded DNGs were added to a dialysis membrane bag (Cellu-Sep T2 MWCO 6000–8000 Da; Membrane Filtration Products Inc., Braine-l'Alleud, Belgium). The dialysis membrane bag was sealed and then immersed in a vial containing fresh phosphate buffer saline (PBS; 25 mL) at different pH values (pH 7.4, 6.8 and 5). The release of DOX from the DNGs was performed under mechanical shaking (100 rpm) at 37 °C using an environmental shaker incubator (model ES-20, Orbital Shaker-Incubator, Biosan, Latvia). At certain time-points, the outer phase of the dialysis membrane bag was harvested and replaced with fresh buffer solution in order to maintain a sink condition for DOX. The DOX concentration in the outer phases was determined under UV/vis absorbance mode at 495 nm.

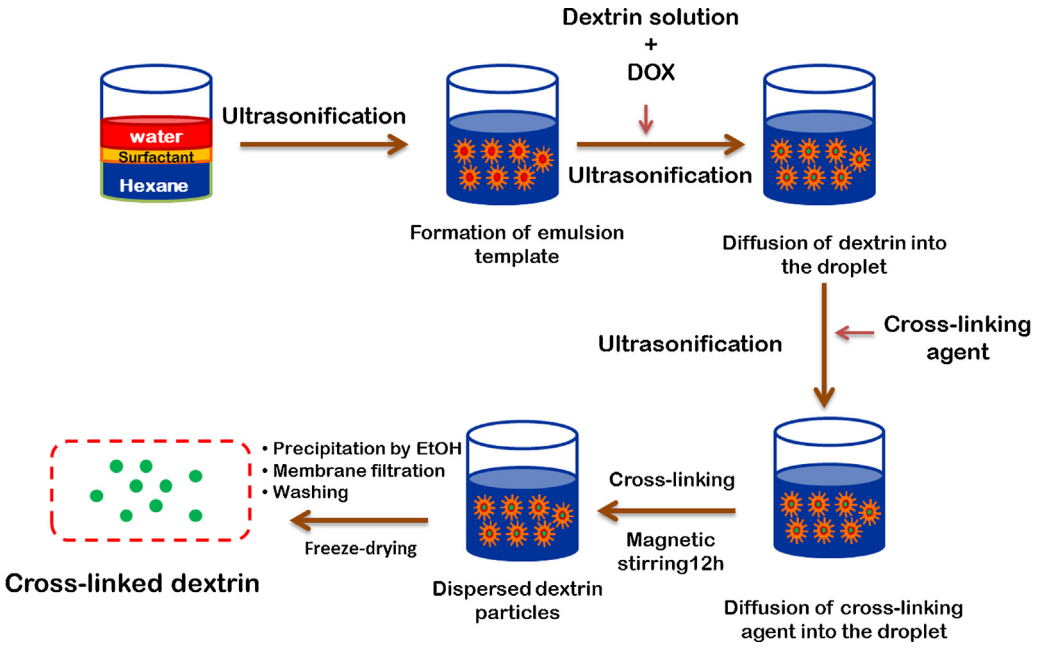

Fig. 1. Schematic of DNG fabrication and pH-dependent drug release.

2.7. Cell culture

Normal murine mesenchymal stem cells (MSCs) and rat cardiomyocyte cell line H9c2 were cultured in Dulbecco's modified Eagle's medium (DMEM) supplemented with 10% heat-inactivated fetal bovine serum (FBS) and 1% penicillin–streptomycin at 37 °C in a CO_2 incubator with 5% CO_2. The cells were harvested with 0.025% trypsin, checked to be at least 90% viable, and then used for assay setup.

2.8. In vitro activity

The *in vitro* cytotoxicity of DOX-loaded DNGs was investigated by determining the cell viability using CellTiter-Blue® assay (Promega, Melbourne, Australia). Briefly, cells were seeded in 96-well plates at a density of 5×10^3 cells/well and incubated in DMEM for 24 h. Then, the medium was replaced by DOX-loaded DNGs or empty DNGs or free DOX samples, diluted in DMEM and incubated for 24 or 48 h. DOX doses of 1 or 5 μM were tested. At given time intervals, CellTiter-Blue® reagent was added and incubated for 30 min in the incubator. The fluorescence intensity was measured by microplate reader (Enspire® 2300, PerkinElmer, Waltham, MA, USA) at E_m 488 nm/E_x 530 nm, in triplicate.

2.9. Fluorescence microscopic determination of cellular uptake

Cellular uptake was observed by an inverted fluorescence microscope (model IX51, Olympus, Tokyo, Japan). For fluorescence

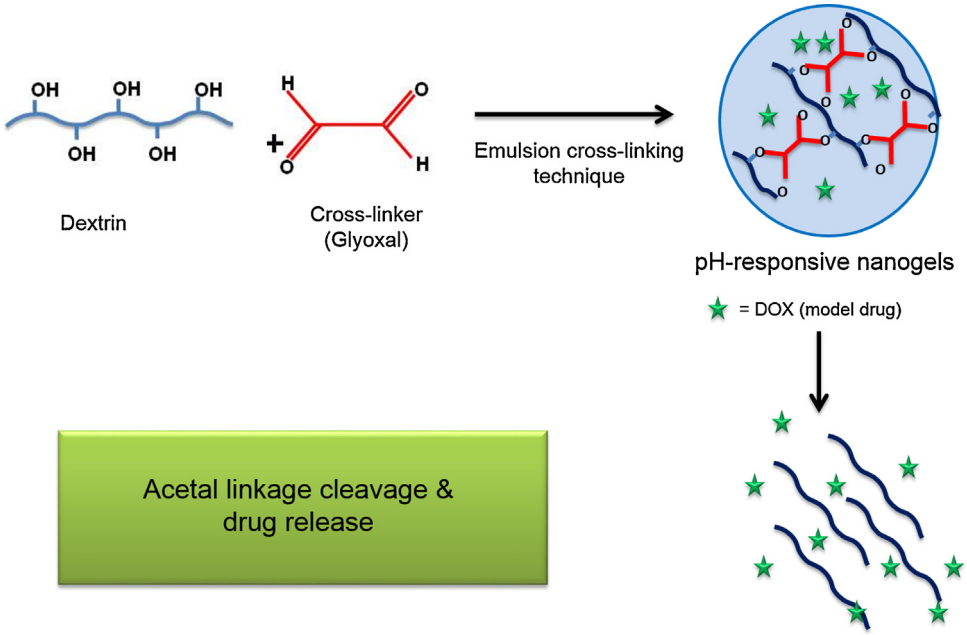

Fig. 2. Schematic of the preparation of pH-responsive nanogels.

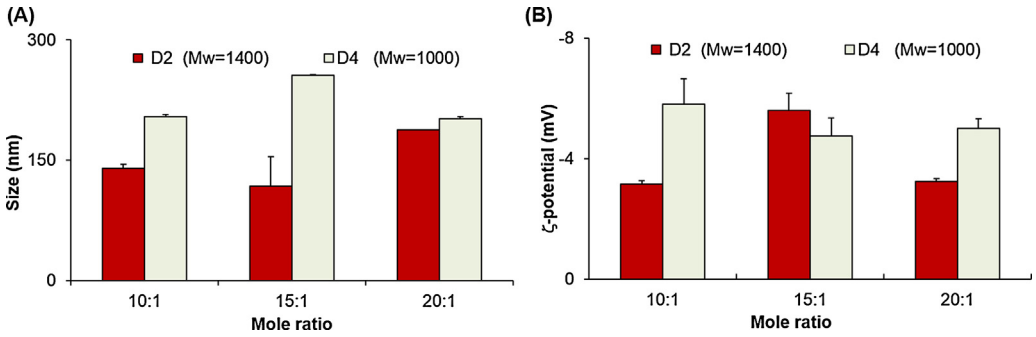

Fig. 3. Effect of molecular weight of dextrin and mole ratio of dextrin to glyoxal on (A) size, and (B) ζ-potential of DNGs ($n = 3$, $p < 0.05$).

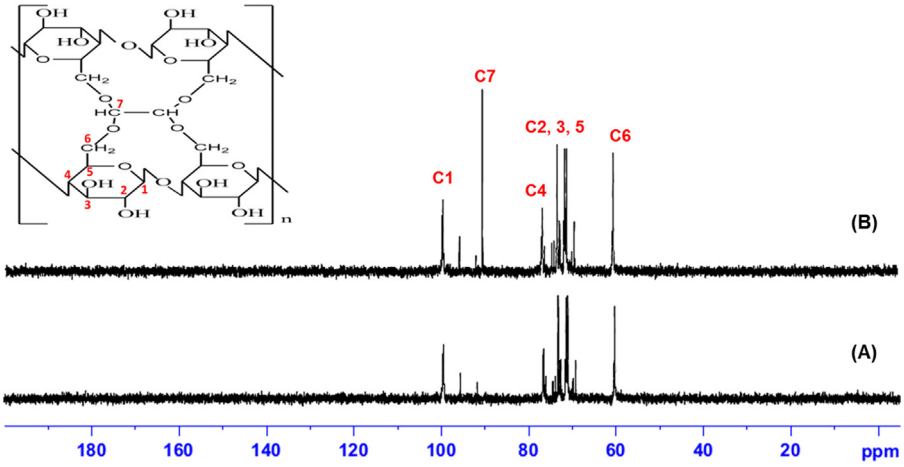

Fig. 4. ^{13}C NMR spectra of (A) native dextrin and (B) DNGs cross-linked by glyoxal at mole ratio of dextrin to glyoxal of 10:1.

microscopic observation, each cell line was seeded in the cell culture dish at a density of 10^5 cells/dish and incubated in free DOX or DOX-loaded DNGs (5 μM DOX equivalent) for different time periods. At given time intervals, the dishes were rinsed twice with PBS (pH 7.4) to remove drug not taken up by the cells. The fluorescent images of cells were acquired on an inverted fluorescence microscope.

2.10. Confocal microscopic determination of cellular uptake

Cells were seeded in a sterile chamber at a concentration of 1×10^5 cells/well in 2.0 mL of complete DMEM and cultured at 37 °C for 24 h and then treated with DOX-loaded DNGs or free DOX at a final DOX concentration of 5 μM for 2, 4 and 8 h. Then, the cells were washed with PBS and incubated at 37 °C for an additional 30 min with 1 μM 4′,6-diamidino-2-phenylindole (DAPI) nuclear counterstain. Thereafter, the cells were washed twice with PBS and fixed with 4% (w/v) formaldehyde in PBS for 30 min at room temperature. The fixed cells were examined under an UltraVIEW® VoX confocal microscope (Waltham, MA, USA) and imaging system with Volocity 6.0.1 software (PerkinElmer, Massachusetts, USA).

2.11. Statistical analysis

Analysis of variance (ANOVA) was performed using SPSS version 11.5 for Windows (SPSS Inc., USA). *Post hoc* testing ($p < 0.05$) of the multiple comparisons was performed by either the Scheffé or Games-Howell test depending on whether Levene's test was insignificant or significant, respectively.

3. Results and discussion

3.1. Fabrication and characterization of pH-responsive DNGs

Nanogels are three-dimensional polymer networks that undergo swelling instead of dissolution in an aqueous environment as a result of the cross-links present in the nano-sized structure. In this study, DNGs were fabricated in w/o nanoemulsion templates using an emulsion cross-linking technique. The aldehyde cross-linking agent, glyoxal, was used to link dextrin chains and form nano-sized droplets of the prepared emulsion template. The hydroxyl groups of dextrin molecules reacted with the carbonyl group of glyoxal to form acid-labile acetal bonds. In order to understand the effect of cross-linker concentration on average diameter,

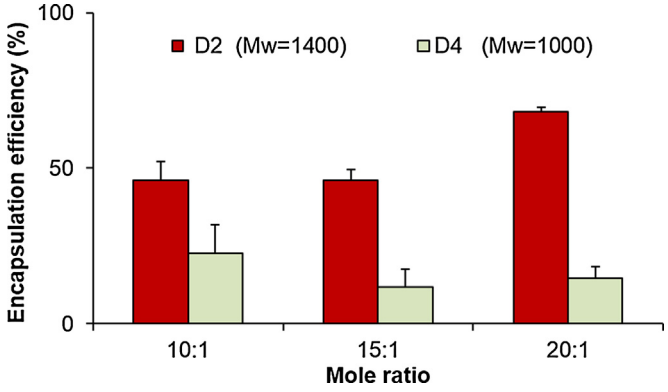

Fig. 5. Encapsulation efficiency of DNGs with different mole ratios of dextrin to glyoxal ($n = 3$, $p < 0.05$).

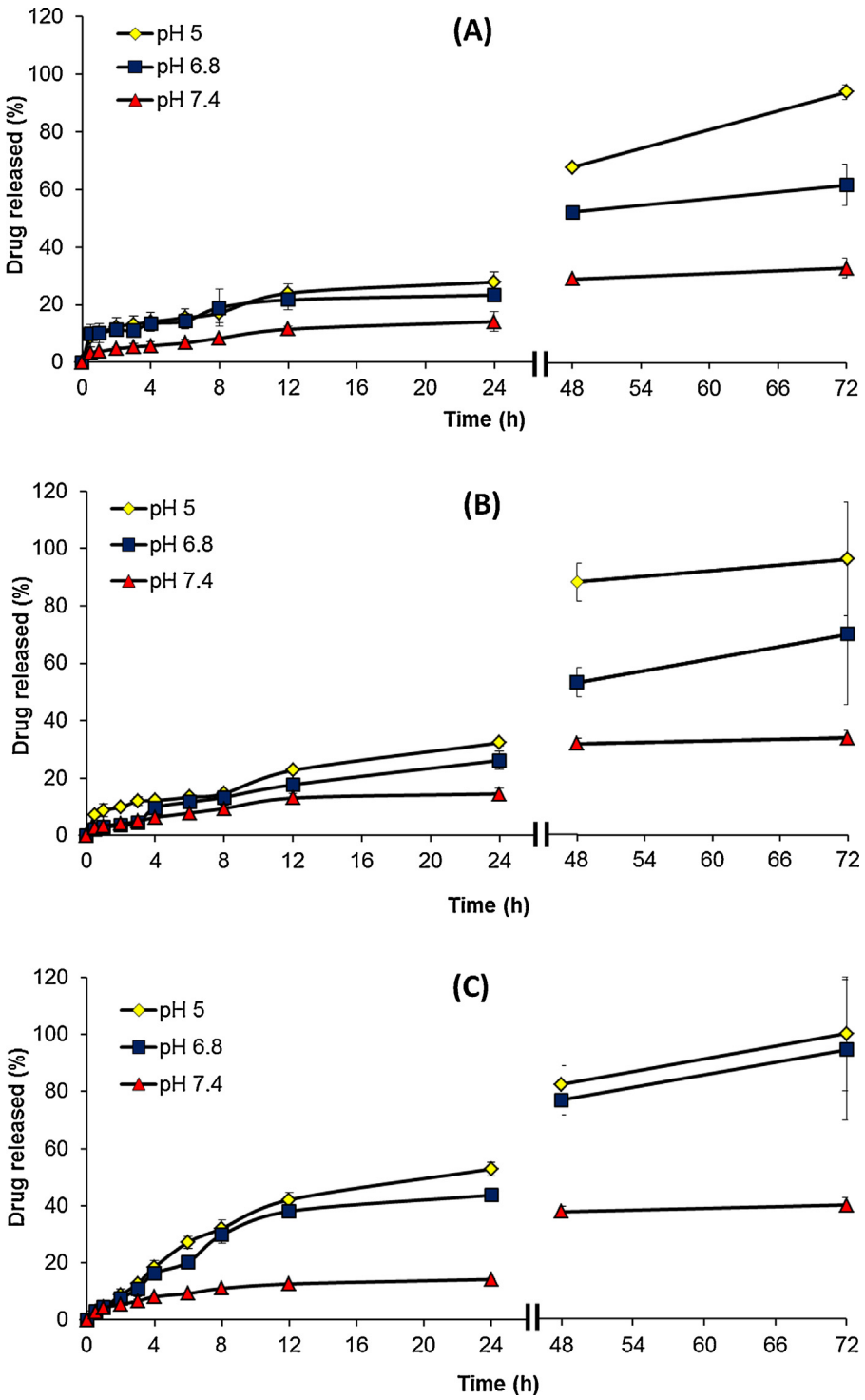

Fig. 6. pH-dependent release profiles of DOX from DNGs with different mole ratios of cross-linker at 37 °C in phosphate buffer; (A) 10:1, (B) 15:1, (C) 20:1.

the mole ratio of dextrin to glyoxal was varied: dextrin:glyoxal of 10:1, 15:1 and 20:1. The hydrodynamic diameter was determined by dynamic light scattering in PBS (pH 7.4).

As shown in Fig. 3, the average diameter of the obtained DNGs showed a significant difference for all mole ratios. Smaller size was achieved when the higher Mw dextrin (D2) was used, as noted previously (Manchun et al., 2014). It is possible that the higher Mw dextrin containing a greater quantity of hydroxyl groups had more interactions with glyoxal and led to an increase in the cross-linking density in the nanoemulsion template. Moreover, for D2, the higher mole ratio of dextrin to glyoxal (20:1), which was the lowest amount of cross-linker, resulted in the larger size of DNGs, compared to the lower ratios (10:1 and 15:1). A decrease in particle size when more cross-linker is incorporated in the polymer network is typically expected of highly cross-linked and condensed networks (Robinson & Peppas, 2002). Interestingly, the DNGs prepared from D4 (lower Mw dextrin) at the mole ratio of dextrin to glyoxal of 15:1 was the largest DNGs (256 nm) while those prepared at other ratios gave the comparable size (~200 nm). The ζ-potential of DNGs showed slightly negative surface charge (−6.52

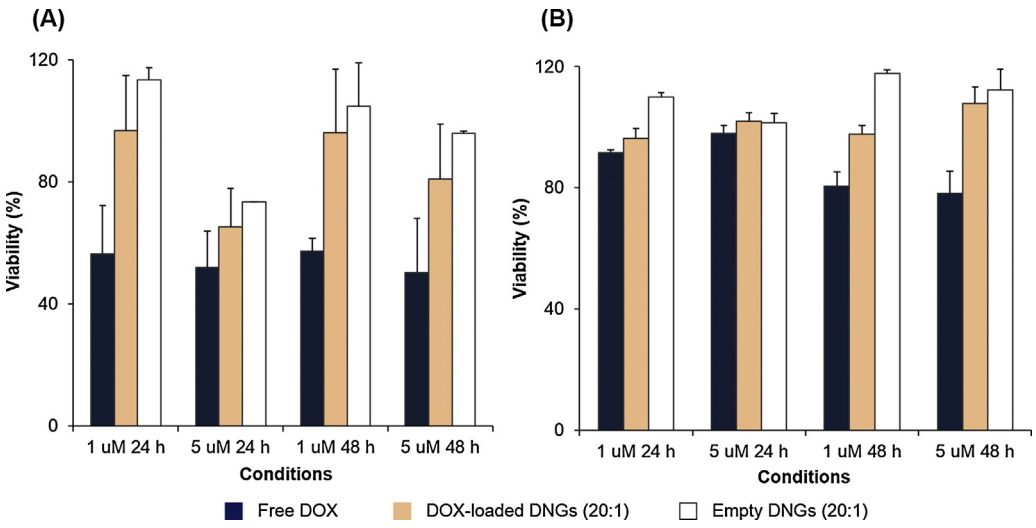

Fig. 7. Cell viability of (A) MSC and (B) H9c2 cells treated with free DOX, DOX-loaded DNG (20:1) and empty DNG (20:1) at various conditions.

to −3.07 mV), due to more hydroxyl groups present on dextrin molecules.

The chemical structure of DNGs was confirmed by ^{13}C NMR. Fig. 4 depicts the chemical shifts of native dextrin and DNGs prepared from D2 at a mole ratio of 10:1. The characteristic chemical shift of native dextrin was assigned to the region between 60 ppm and 100 ppm for the carbons of dextrin (Fig. 4A). The chemical shifts at 99.52 ppm (C1), 76.62 ppm (C4), 73.27–71.10 ppm (C2, C3, C5), and 60.39 ppm (C6) verified presence of dextrin molecule as identified previously (Carvalho et al., 2007; Hu et al., 2013; Liu et al., 2011). After cross-linking, the additional signal at 90.44 ppm (C7) that appeared in the ^{13}C NMR of DNGs (Fig. 4B) was attributed to the carbon atom of glyoxal.

3.2. Doxorubicin loading

DOX was introduced into the DNGs during cross-linking of dextrin chains which formed the nanogel structure, resulting in drug incorporation and immobilization within the nanogels. The drug content and loading efficiency were investigated by a direct method. Nanogels were dissolved in 1.0 N HCl in order to break the acetal bonds, resulting in the disruption of nanogel structure and subsequent release of DOX. The encapsulation efficiency is shown in Fig. 5 for each type of dextrin and mole ratio of dextrin to glyoxal. DNGs made of D2 showed significantly higher encapsulation efficiency than those made of D4. This is probably due to the fact that dextrin with a higher molecular weight led to an increase in the cross-linking density, resulting in higher encapsulation efficiency. Furthermore, the encapsulation efficiency of DOX in the DNGs made of D2 was found to increase with a decrease in the mole ratio of dextrin to glyoxal. The cross-linking density might be decreased when mole ratio of dextrin to glyoxal is decreased, causing an increase in the number of cavities in the DNG structure. In contrast, for DNGs made of D4, a significant decrease ($p < 0.05$) in encapsulation efficiency was observed when mole ratio of dextrin to glyoxal was decreased. This is because the amount of cross-linker is insufficient to completely link dextrin chains so as to form a nanogel structure.

3.3. pH-dependent release of DOX

The *in vitro* release profiles of DOX from DNGs made of D2 at various mole ratios of dextrin to glyoxal (10:1, 15:1 and 20:1) as function of pH (5, 6.8 and 7.4) were investigated, as shown in Fig. 6. The release of DOX from DNGs increased with decreasing medium pH. The amount of cross-linker also showed an important effect on modulating drug release patterns of DNGs. The percent drug release increased as the amount of cross-linker decreased. At the mole ratio of dextrin to glyoxal of 20:1 (Fig. 6C), about 14%, 44%, 53% of DOX was released within 24 h and about 40%, 94%, 100% of DOX was released within 72 h from DNGs at pH 7.4, 6.8 and 5, respectively. The difference in drug release behavior at different pHs was mainly attributed to the breaking of acetal linkages in the DNGs. In acidic condition, acetal bonds are expected to hydrolyze, resulting in destabilization of the DNG structure that would accelerate DOX release. Release at pH 5.0 and 6.8 was significantly higher than that at pH 7.4, attributing to the increased hydrolysis of acetal linkage in an acidic environment (Knorr, Allmendinger, Walker, Paintner, & Wagner, 2007). The slower release rate at pH 7.4 for all DNGs suggested that slight changes in DNG structure had occurred. Compared to the normal tissue pH (7.4), pH values of intracellular compartments, that is, endosomes and lysosomes lie between 4.5 and 6.5 and average extracellular pH values in tumor tissues is 6.8 (Manchun, Dass, & Sriamornsak, 2012), thus the DNGs could negate the undesirable toxicity associated with the free drug in normal tissue.

At the same pH, release increased as the mole ratio of dextrin to glyoxal increased. For instance, at pH 6.8, the percentage DOX released from lower mole ratios of dextrin to glyoxal (10:1 and 15:1) was approximately 62% and 70% within 72 h, respectively, compared to 94% for that of higher ratio (20:1). A higher drug release was observed when the pH of the medium was further decreased to pH 5.0. About 94%, 96% and 100% of drug were released within 72 h from DNGs prepared at mole ratio of dextrin to glyoxal of 10:1, 15:1 and 20:1, respectively.

It is interesting that DOX release from DNGs prepared at the lower mole ratios of dextrin to glyoxal (that is, 10:1 and 15:1) was biphasic while that of 20:1 was monophasic, as shown in Fig. 6. It is well-known that drug release is also affected by the cross-linking density of the nanogels. Since the mesh size of the nanogels with mole ratio of 10:1 and 15:1 was smaller, it became difficult for DOX molecules to embed inside the nanogel structure, and therefore, drug molecules were also located at the outer layer of nanogels. The DOX in the outer layer is believed to be released as the first pulse (burst release), while the second (protracted) phase of the release is controlled by the rate of DOX release from the actual matrix of the DNGs. In case of the DNG prepared at the higher mole ratio of dextrin to glyoxal (20:1), the available cross-linker was lower which resulted in a larger mesh size of the DNGs. This resulted

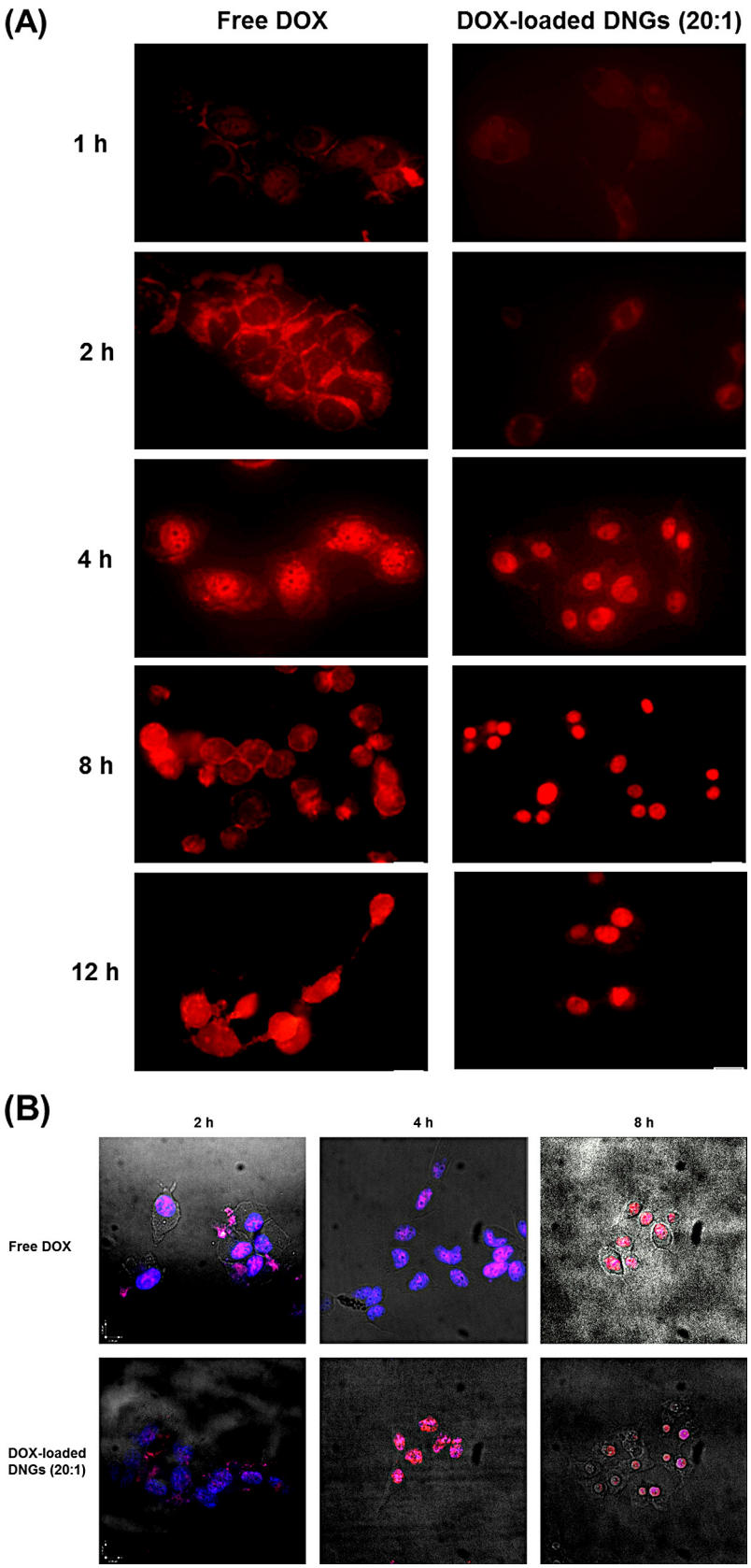

Fig. 8. Cellular uptake of free DOX and DOX-loaded DNGs (20:1) in human colorectal cancer HT29 cells as determined by (A) fluorescence microscopy and (B) confocal microscopy.

in the high diffusivity of DOX from the DNGs which exhibited a monophasic release pattern.

3.4. In vitro anticancer activity and cellular uptake

The cytotoxicity of the free DOX, DOX-loaded DNGs and empty DNGs against normal cells (MSC and H9c2) was investigated. DNGs made from D2, prepared at the mole ratio of dextrin to glyoxal of 20:1 were selected for further study due to its optimal drug loading and release kinetics. The cells were incubated with free DOX or DOX-loaded DNGs (for 24 and 48 h). In this study, different amounts of DOX-loaded DNGs equivalent to 1 and 5 μM DOX were used, that is, 3.7 mg for 1 μM and 18.3 mg for 5 μM were dissolved in 1 mL of PBS. The empty DNGs were used for comparison, at the equivalent amount of DNGs to that of DOX-loaded DNGs. Cardiotoxicity due to free DOX is a commonly encountered problem clinically (Tacar & Dass, 2013). To this end, a commonly tested cell line for cardiomyocytes, H9c2, was tested, alongside primary cells for MSCs. Due to DOX's antiproliferative activity, stem cells could be particularly vulnerable to its cytotoxicity. The empty DNGs were practically non-toxic in normal MSC and H9c2 cells (Fig. 7), and more importantly, the cytotoxic action of DOX was consistently reduced when nanoencapsulated within DNGs between the 24 and 48 h incubations, and at the two doses of DOX – 1 and 5 μM.

The intracellular distribution of free DOX and DOX-loaded DNGs prepared at the mole ratio of dextrin to glyoxal of 20:1 (equivalent to 5 μM DOX) was investigated using fluorescence microscopy (Fig. 8A). Free DOX and DOX-loaded DNGs were distributed in the cytoplasm region within 1 h of incubation and localized in the nucleus after 4 h and 8 h incubation with free DOX and DOX-loaded DNGs, respectively. Intense fluorescence was exhibited after 8 h incubation with DOX-loaded DNGs, particular in the nucleus. This was confirmed with confocal microscopy, which indicated that DNGs facilitated the fast drug release after cellular uptake at 4 h incubation (Fig. 8B). This is probably due to various routes of cellular internalization. Free DOX molecules are transported into cells by passive diffusion (Chiang et al., 2012; Shuai, Ai, Nasongkla, Kim, & Gao, 2004) whereas DOX-loaded DNGs should be internalized *via* non-specific endocytosis. These cellular uptake profiles of DOX molecules are likely due to the rapid destabilization of the DOX-loaded DNGs under weakly acidic intracellular conditions, leading to the rapid release of DOX from DNGs and subsequent translocation to the nucleus. These findings suggest that DOX-loaded DNGs are suitable for selective delivery of drug payloads to the acidic extracellular environment of tumors, and furthermore, particularly being capable of drug release within cells once cellular uptake has occurred. In addition, these DNGs are ideal for drugs that need to be delivered to the nucleus for anticancer activity.

4. Conclusion

pH-responsive DNGs were successfully fabricated by a simple emulsion cross-linking technique. Molecular weight of dextrin and mole ratio of dextrin to glyoxal affected physical properties and drug encapsulation efficiency. The fastest DOX release from DOX-loaded DNGs occurred at pH 5 (endosomal pH) while at physiological pH (pH 7.4), DOX release was the slowest. DOX-loaded DNGs localized to the nucleus of human tumor cells. DNG encapsulation significantly reduced DOX toxicity to normal (non-tumor) cells such as cardiomyocytes and MSCs. These results suggest that the pH-responsive DNGs may be an effective intracellular drug delivery system for DOX cancer therapy, and one that is capable of reducing side-effects of this anthracycline drug, particularly in the heart.

Acknowledgements

The authors acknowledge the Royal Golden Jubilee Ph.D. Program (grant number PHD/0361/2551) and Research Promotion in Higher Education Scheme from Commission of Higher Education (Thailand) for the financial support. Thanks to Siam Modified Starch Company, Ltd. (Pathumthani, Thailand) who kindly supplied dextrin samples. The authors also thank Ms. Mina Elahy and staff at the Biosciences Research Precinct (Australia). CRD is supported by a Curtin Academic50 grant scheme.

References

Alexis, F., Pridgen, E., Langer, R., & Farokhzad, O. (2010). *Nanoparticle technologies for cancer therapy. Drug delivery*. Berlin/Heidelberg: Springer.

Arif, I. S., Hooper, C. L., Greco, F., Williams, A. C., & Boateng, S. Y. (2013). Increasing doxorubicin activity against breast cancer cells using PPARγ-ligands and by exploiting circadian rhythms. *British Journal of Pharmacology*, *169*(5), 1178–1188.

Bachelder, E. M., Beaudette, T. T., Broaders, K. E., Dashe, J., & Frèchet, J. M. J. (2008). Acetal-derivatized dextran: An acid-responsive biodegradable material for therapeutic applications. *Journal of the American Chemical Society*, *130*(32), 10494–10495.

Bae, Y., Fukushima, S., Harada, A., & Kataoka, K. (2003). Design of environment-sensitive supramolecular assemblies for intracellular drug delivery: Polymeric micelles that are responsive to intracellular pH change. *Angewandte Chemie International Edition*, *42*(38), 4640–4643.

Bae, Y., Nishiyama, N., & Kataoka, K. (2007). In vivo antitumor activity of the folate-conjugated pH-sensitive polymeric micelle selectively releasing adriamycin in the intracellular acidic compartments. *Bioconjugate Chemistry*, *18*(4), 1131–1139.

Carvalho, J., Gonçalves, C., Gil, A. M., & Gama, F. M. (2007). Production and characterization of a new dextrin based hydrogel. *European Polymer Journal*, *43*(7), 3050–3059.

Chiang, W.-H., Ho, V. T., Huang, W.-C., Huang, Y.-F., Chern, C.-S., & Chiu, H.-C. (2012). Dual stimuli-responsive polymeric hollow nanogels designed as carriers for intracellular triggered drug release. *Langmuir*, *28*(42), 15056–15064.

Ferguson, E. L., & Duncan, R. (2009). Dextrin-phospholipase A2: Synthesis and evaluation as a bioresponsive anticancer conjugate. *Biomacromolecules*, *10*(6), 1358–1364.

Fleige, E., Quadir, M. A., & Haag, R. (2012). Stimuli-responsive polymeric nanocarriers for the controlled transport of active compounds: Concepts and applications. *Advanced Drug Delivery Reviews*, *64*(9), 866–884.

Ganta, S., Devalapally, H., Shahiwala, A., & Amiji, M. (2008). A review of stimuli-responsive nanocarriers for drug and gene delivery. *Journal of Controlled Release*, *126*(3), 187–204.

Gerweck, L. E., & Seetharaman, K. (1996). Cellular pH gradient in tumor versus normal tissue: Potential exploitation for the treatment of cancer. *Cancer Research*, *56*(6), 1194–1198.

Gianni, L., Herman, E. H., Lipshultz, S. E., Minotti, G., Sarvazyan, N., & Sawyer, D. B. (2008). Anthracycline cardiotoxicity: From bench to bedside. *Journal of Clinical Oncology*, *26*(22), 3777–3784.

Gonçalves, C., & Gama, F. M. (2008). Characterization of the self-assembly process of hydrophobically modified dextrin. *European Polymer Journal*, *44*(11), 3529–3534.

Gonçalves, C., Martins, J. A., & Gama, F. M. (2007). Self-assembled nanoparticles of dextrin substituted with hexadecanethiol. *Biomacromolecules*, *8*(2), 392–398.

Gonçalves, C., Pereira, P., Schellenberg, P., Coutinho, P. J., & Gama, M. (2012). Self-assembled dextrin nanogel as curcumin delivery system. *Journal of Biomaterials and Nanobiotechnology*, *3*(2), 178–184.

Gonçalves, C., Torrado, E., Martins, T., Pereira, P., Pedrosa, J., & Gama, M. (2010). Dextrin nanoparticles: Studies on the interaction with murine macrophages and blood clearance. *Colloids and Surfaces B: Biointerfaces*, *75*(2), 483–489.

Hu, F.-Q., Liu, L.-N., Du, Y.-Z., & Yuan, H. (2009). Synthesis and antitumor activity of doxorubicin conjugated stearic acid-g-chitosan oligosaccharide polymeric micelles. *Biomaterials*, *30*(36), 6955–6963.

Hu, X., Wei, B., Zhang, B., Xu, X., Jin, Z., & Tian, Y. (2013). Synthesis and characterization of dextrin monosuccinate. *Carbohydrate Polymers*, *97*(1), 111–115.

Knorr, V., Allmendinger, L., Walker, G. F., Paintner, F. F., & Wagner, E. (2007). An acetal-based PEGylation reagent for pH-sensitive shielding of DNA polyplexes. *Bioconjugate Chemistry*, *18*(4), 1218–1225.

Liu, X., Wang, Y., Cao, Y., Yadama, V., Xian, M., & Zhang, J. (2011). Study of dextrin-derived curing agent for waterborne epoxy adhesive. *Carbohydrate Polymers*, *83*(3), 1180–1184.

Maeda, H., Bharate, G. Y., & Daruwalla, J. (2009). Polymeric drugs for efficient tumor-targeted drug delivery based on EPR-effect. *European Journal of Pharmaceutics and Biopharmaceutics*, *71*(3), 409–419.

Maeda, H., Sawa, T., & Konno, T. (2001). Mechanism of tumor-targeted delivery of macromolecular drugs, including the EPR effect in solid tumor and clinical overview of the prototype polymeric drug SMANCS. *Journal of Controlled Release*, *74*(1-3), 47–61.

Manchun, S., Dass, C. R., & Sriamornsak, P. (2012). Targeted therapy for cancer using pH-responsive nanocarrier systems. *Life Sciences*, *90*(11–12), 381–387.

Manchun, S., Dass, C. R., & Sriamornsak, P. (2014). Designing nanoemulsion templates for fabrication of dextrin nanoparticles via emulsion cross-linking technique. *Carbohydrate Polymers*, *101*, 650–655.

Minotti, G., Menna, P., Salvatorelli, E., Cairo, G., & Gianni, L. (2004). Anthracyclines: Molecular advances and pharmacologic developments in antitumor activity and cardiotoxicity. *Pharmacological Reviews*, *56*(2), 185–229.

Motornov, M., Roiter, Y., Tokarev, I., & Minko, S. (2010). Stimuli-responsive nanoparticles, nanogels and capsules for integrated multifunctional intelligent systems. *Progress in Polymer Science*, *35*(1–2), 174–211.

Robinson, D. N., & Peppas, N. A. (2002). Preparation and characterization of pH-responsive poly(methacrylic acid-g-ethylene glycol) nanospheres. *Macromolecules*, *35*(9), 3668–3674.

Shi, J., Votruba, A. R., Farokhzad, O. C., & Langer, R. (2010). Nanotechnology in drug delivery and tissue engineering: From discovery to applications. *Nano Letters*, *10*(9), 3223–3230.

Shuai, X., Ai, H., Nasongkla, N., Kim, S., & Gao, J. (2004). Micellar carriers based on block copolymers of poly(Îμ-caprolactone) and poly(ethylene glycol) for doxorubicin delivery. *Journal of Controlled Release*, *98*(3), 415–426.

Soleimani, M., & Nadri, S. (2009). A protocol for isolation and culture of mesenchymal stem cells from mouse bone marrow. *Nature Protocols*, *4*(1), 102–106.

Tacar, O., & Dass, C. R. (2013). Doxorubicin-induced death in tumour cells and cardiomyocytes: Is autophagy the key to improving future clinical outcomes? *Journal of Pharmacy and Pharmacology*, *65*(11), 1577–1589.

Tacar, O., Sriamornsak, P., & Dass, C. R. (2013). Doxorubicin: An update on anticancer molecular action, toxicity and novel drug delivery systems. *Journal of Pharmacy and Pharmacology*, *65*(2), 157–170.

Weng, L., Le, H. C., Lin, J., & Golzarian, J. (2011). Doxorubicin loading and eluting characteristics of bioresorbable hydrogel microspheres: In vitro study. *International Journal of Pharmaceutics*, *409*(1–2), 185–193.

Yoo, H. S., Lee, E. A., & Park, T. G. (2002). Doxorubicin-conjugated biodegradable polymeric micelles having acid-cleavable linkages. *Journal of Controlled Release*, *82*(1), 17–27.